JOURNAL OF GEOPHYSICAL RESEARCH, VOL. 99, NO. A12, PAGES 23,571–23,582, DECEMBER 1, 1994

Hybrid state of the tail magnetic configuration during steady convection events

V. A. Sergeev,[1] T. I. Pulkkinen, and R. J. Pellinen
Finnish Meteorological Institute, Helsinki

N. A. Tsyganenko[1]
NASA Goddard Space Flight Center, Greenbelt, Maryland

Abstract. Previous observations have shown that during periods of steady magnetospheric convection (SMC) a large amount of magnetic flux crosses the plasma sheet (corresponding to ~10° wide auroral oval at the nightside) and that the magnetic configuration in the midtail is relaxed (the current sheet is thick and contains enhanced B_Z). These signatures are typical for the substorm recovery phase. Using near-geostationary magnetic field data, magnetic field modeling, and a novel diagnostic technique (isotropic boundary algorithm), we show that in the near-Earth tail the magnetic configuration is very stretched during the SMC events. This stretching is caused by an intense, thin westward current. Because of the strongly depressed B_Z, there is a large radial gradient in the near-tail magnetic field. These signatures have been previously associated only with the substorm growth phase. Our results indicate that during the SMC periods the magnetic configuration is very peculiar, with co-existing thin near-Earth current sheet and thick midtail plasma sheet. The deep local minimum of the equatorial B_Z that develops at $R \sim 12\ R_E$ is consistent with steady, adiabatic, Earthward convection in the midtail. These results impose constraints on the existing substorm theories, and call for an explanation of how such a stressed configuration can persist for such a long time without tail current disruptions that occur at the end of a substorm growth phase.

Introduction

Erickson and Wolf [1980] were first to formulate the so-called "pressure balance inconsistency" (PBI) problem for the magnetotail plasma sheet. The problem, which has later been confirmed by theoretical analyses and numerical simulations [*Erickson*, 1992], is that homogeneous, steady, Earthward convection of closed magnetic flux tubes in a taillike mangetic field configuration leads to plasma heating and compression so strong that the resulting plasma distribution cannot be in pressure balance with the magnetic field. Steady state solutions based on the adiabatic "slow flow" magnetohydrodynamic (MHD) approximation can be constructed [*Hau et al.*, 1989; *Hau*, 1991], but they require a deep local minimum of the magnetic field (of only a few nanoteslas) in the current sheet near the inner edge of the plasma sheet. The existence of such a minimum is not in agreement with the monotonous tailward decrease of B_Z in all magnetospheric models, and has not been found in statistical studies of the tail magnetic field. (The *Tsyganenko* [1989a] models show a small minimum at $X \sim -20\ R_E$, but this is too small and too smooth to contribute to this effect.) This together with results that the minimum B_Z region may be unstable to the tearing instability, led Hau et al. to conclude that such equilibria would not be probable in the real magnetosphere.

Several mechanisms have been discussed to provide the reduced heating and compression during Earthward convection. These include finite tail width effects [*Tsyganenko*, 1982; *Spence and Kivelson*, 1990], small-scale plasma inhomogeneities (the "bubble" mechanism by *Pontius and Wolf* [1990]), kinetic effects [*Ashour-Abdalla et al.*, 1992], and the three-dimensional nature of convection and the magnetic configuration [*Sergeev and Lennartsson*, 1988; *Sergeev et al.*, 1990]. None of these effects proved to be strong enough to resolve the pressure balance inconsistency for the steady state. In the average tail configuration with the externally imposed dawn-to-dusk electric field, steady convection leads to a time-dependent global evolution of the magnetotail, including tailward stretching of the magnetic

[1]Institute of Physics, University of St. Petersburg, St. Petersburg, Russia.

Paper number 94JA01980.
0148-0227/94/94JA-01980$05.00

field lines and large field depression in the near-Earth equatorial magnetosphere caused by the growing tail current. This model (referred to henceforth as the PBI substorm model) nicely describes the observations during the substorm growth phase (cf. extended discussion by *Erickson* [1992]).

The applicability of the PBI substorm model is, however, questioned by the existence of the (rare) events of steady convection during the (rare) events of very steady solar wind flow and southward interplanetary magnetic field (IMF). In these cases, enhanced convection may continue for up to 10 hours without substorm signatures. These "steady magnetospheric convection" (SMC) events are characterized by intense Earthward convection (seen both in the ionosphere and in the plasma sheet) as well as by the large-scale stability of both the tail magnetic field and the auroral oval (cf. *Sergeev and Lennartsson* [1988] and *Yahnin et al.*, [1994] for observations in the plasma sheet and ionosphere, respectively).

The identification of the steady magnetospheric convection events has been discussed in several papers [*Sergeev and Lennartsson*, 1988; *Yahnin et al.*, 1994]; here we will only briefly mention their most important signatures: SMC events are relatively long time periods (at least 4–6 hours, or several typical substorm timescales) characterized by steady solar wind flow carrying southward IMF, by the presence of enhanced convection (evidenced, for example, by enhanced auroral electrojet (AU/AL) indices) and by the absence of usual substorm signatures (either on the ground or in the near-Earth tail or midtail). Typically, an SMC event starts after one substorm and ends with another, thus representing a long, active interval between two substorms.

This paper focuses on comparison of observations during steady magnetospheric convection events and the equilibrium models of *Hau et al.* [1989] that support steady convection. It is shown that during SMC events, the tail may, indeed, develop to a state which contains the B_Z minimum predicted by the PBI substorm model. The main characteristic to be studied is the actual (rather than the average) plasma sheet magnetic field configuration, which governs the plasma compression and heating during the Earthward convection. The two regions of interest are the near-Earth tail (5–15 R_E) and the midtail (15–30 R_E). In this paper we will concentrate on the near-Earth tail observations utilizing data from the GOES and Active Magnetospheric Patricle Trace Explorer (AMPTE/CCE) spacecraft and a novel remote sensing technique to monitor the equatorial magnetic field (the isotropic boundary algorithm, described and tested by *Sergeev et al.* [1993]). The midtail characteristics are inferred from previous work by *Sergeev and Lennartsson* [1988]. We also present a first attempt to model the observed magnetic configuration during one SMC event and conclude by discussing the results in relation to the applicability of the PBI substorm model.

Near-Equatorial Magnetic Field Observations

A period of steady magnetospheric convection, which lasted for more than 10 hours (13 hours between two substorms), occurred on November 24, 1981. This event has been discussed in detail by *Yahnin et al.* [1994]. The large-scale stability of the auroral oval between 0300 and 1200 UT that day was confirmed by DE 1 imager data and low-altitude NOAA spacecraft particle data (the latter will be described in the following section). Most activity indices showed moderate level of disturbance (Kp varied between 2– and 2+, AE was about 300–400 nT, the IMF B_Z was about −4 nT, and the solar wind dynamic pressure was about 0.7 nPa). However, the Dst index was steadily at about −60 nT, and the nightside geosynchronous magnetic field was strongly disturbed.

Figure 1 shows magnetic field observations made by GOES 2, which was located at 6.6 R_E, 108°W geographic longitude. The satellite crossed the local magnetic midnight at 0712 UT about 0.5 R_E above the current sheet. The data are presented in a local geographic coordinate system in which V is measured along the Earth-satellite line (positive Earthward), H is northward (in the geographic meridional plane) and D is eastward, thus completing the triad. The dotted and dashed lines give the magnetic field predicted by the Tsyganenko [1989a] (T89) models for $Kp = 3$ and $Kp = 5$, respectively. No significant substormlike varia-

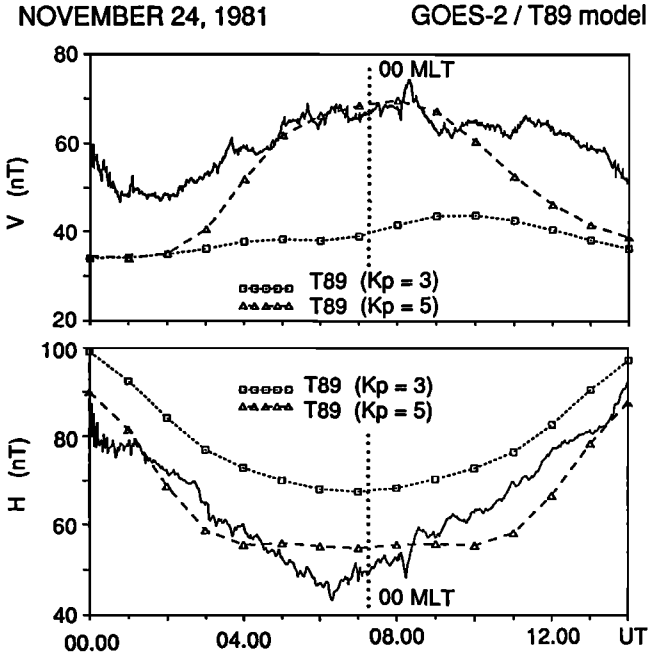

Figure 1. Magnetic field measurements in geographic coordinates (H (vertical) and V (radial) components) measured by GOES 2 on November 24, 1981. The dotted and dashed lines show the field values computed using the T89 models for $Kp = 3$ and $Kp = 5$, respectively. Local midnight at GOES 2 is at 0710 UT.

tions were observed during the entire period. However, the magnetic field was very taillike (the radial component (V) was enhanced, and the vertical (H) component was strongly depressed). The tail stretching at midnight is comparable to or even larger than the $Kp = 5$ (most disturbed) version of the T89 model. The data are not in agreement with the T89 model outside of the 2200–0200 MLT sector (0500–0900 UT), where even the $Kp = 5$ model was unable to predict the observed large radial component. The last observation implies that the intense current sheet that stretches the field was aligned azimuthally (westward), rather than in the dawn-dusk direction. Such a current system has been previously reported in connection with strong substorm growth phase activity [*Pulkkinen et al.*, 1991].

We looked through several cases where geosynchronous magnetic field observations were available during the SMC events. Typically, the magnetic field was found to be very taillike and the H component was very small. The degree of tailward stretching was much larger than one would normally expect from the level of ionospheric electrojet activity. Here we show one example of very stretched near-tail magnetic field to show how large this depression can be for more disturbed SMC events. During November 25, 1986, 0000–0800 UT (the interval started during the previous day and ended with a substorm expansion onset at about 0740 UT), Kp was about 5, the AE index varied between 500 and 700 nT, IMF had a southward component of about 4–6 nT, and the solar wind dynamic pressure was about 3 nPa. Again, the Dst index was rather disturbed, in this case it was about −80 nT.

Figure 2 shows the magnetic field data from GOES 5 and GOES 6 during the November 25, 1986, event. The lines marked with squares and triangles give the T89 model field for $Kp = 5$. Note that during the winter season the GOES spacecraft are close to the current sheet center. (The distance from the current sheet central surface in the T89 model to the GOES spacecraft was about 0.5 R_E for this case.) The radial component at both GOES 5 and GOES 6 close to midnight was comparable to that given by the T89 model for $Kp = 5$, and the field depression in the H component was smaller than the model value by 20–40 nT. The results are qualitatively consistent with a very intense and thin current sheet near the geosynchronous distance, resembling conditions during the substorm growth phase. Note that this event has not been studied using as many complementary data as were available during the November 24, 1981 event, and thus we cannot completely rule out the possibility of a weak substorm-like activity. However, we would like to emphasize that in the SMC events we

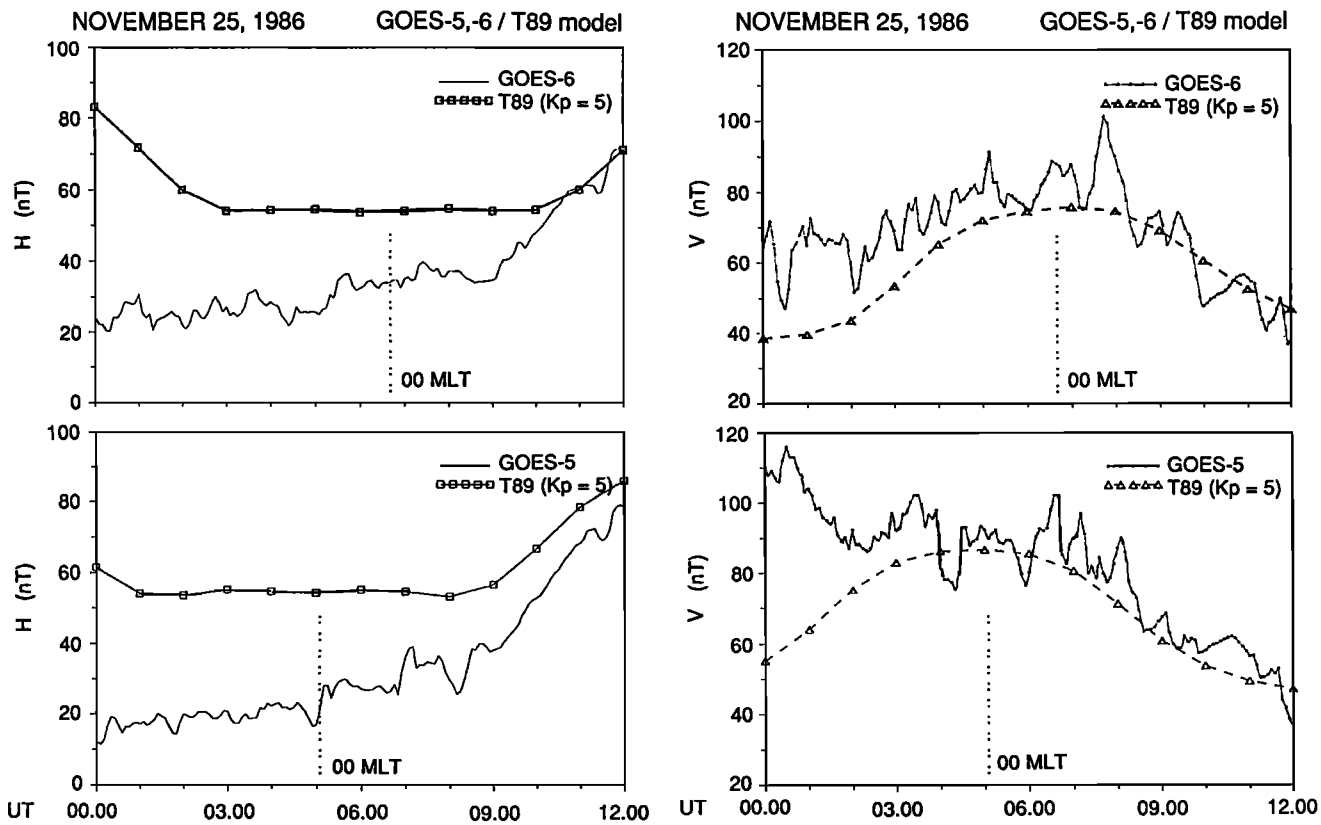

Figure 2. Magnetic field vertical (H) component in geographic coordinates measured by GOES 5 and GOES 6 on November 25, 1986. The local magnetic midnight is at about 0500 UT and 0700 UT at GOES 5 and GOES 6, respectively. The local midnights are shown by the dotted vertical lines.

have studied there were no signatures of current disruptions in the near-Earth tail that would destroy the stressed magnetic configuration.

In order to estimate the current sheet thickness and evaluate the actual field magnitude at the current sheet center, we searched the AMPTE/CCE database during periods when it crossed the current sheet plane in the nightside. We found several current sheet crossings that occurred during SMC-like events; one moderate SMC event occurred during 1600–2300 UT on January 25, 1988. After 1500 UT that day the solar wind flow was very stable, the IMF had a southward component of about −4 nT, the solar wind dynamic pressure was about 2.6 nPa, Kp varied between 1+ to 2−, and the approximate value of AE was around 200 nT. (AE was estimated from available auroral zone magnetograms. The absence of substorms was checked by using data from the EISCAT magnetometer cross in Scandinavia, which during that time scanned the midnight sector.) Between 1800 and 2300 UT no signatures of substorm activations were found in the ground data studied (including auroral zone magnetic and auroral data, mid-latitude magnetic variations, and Pi2 pulsations). Dst was about −20 nT during this event.

To better compare the actual and model magnetic fields, the field values with the dipole field subtracted ($\delta B_X, \delta B_Y, \delta B_Z$) are plotted in Figure 3a. The lowest panel shows the actual measured B_Z profile. AMPTE /CCE crossed the current sheet center (as indicated by the change of sign of both B_X and B_Y) between 2100 and 2200 UT close to its apogee (8.8 R_E) at 2130 MLT. During this crossing the total field value (approximately equal to the B_Z value in the current sheet center) was only about 5–7 nT, which is an extremely low value for this distance. Few events where $B_{TOT} \sim 10$ nT have been previously found just at the end of the growth phase [*Fairfield and Zanetti*, 1989; *Lui et al.*, 1992]. Clearly, this was not a short-term transient variation because a similar large depression ($\delta B_Z \simeq -40$ nT, twice as large as that given by the T89, $Kp = 5$ model) was seen during 5 hours after 1900 UT.

Between 1930 UT and 2230 UT there was a well-defined, approximately linear variation of both B_X and B_Y. To visualize the spatial scale, Figure 3b shows the magnetic field as a function of distance from the current sheet. The distance from the current sheet ($\delta Z_{NS} = Z - Z_{NS}$) was calculated using the warped current sheet in the T89 model for $Kp = 5$. Outside

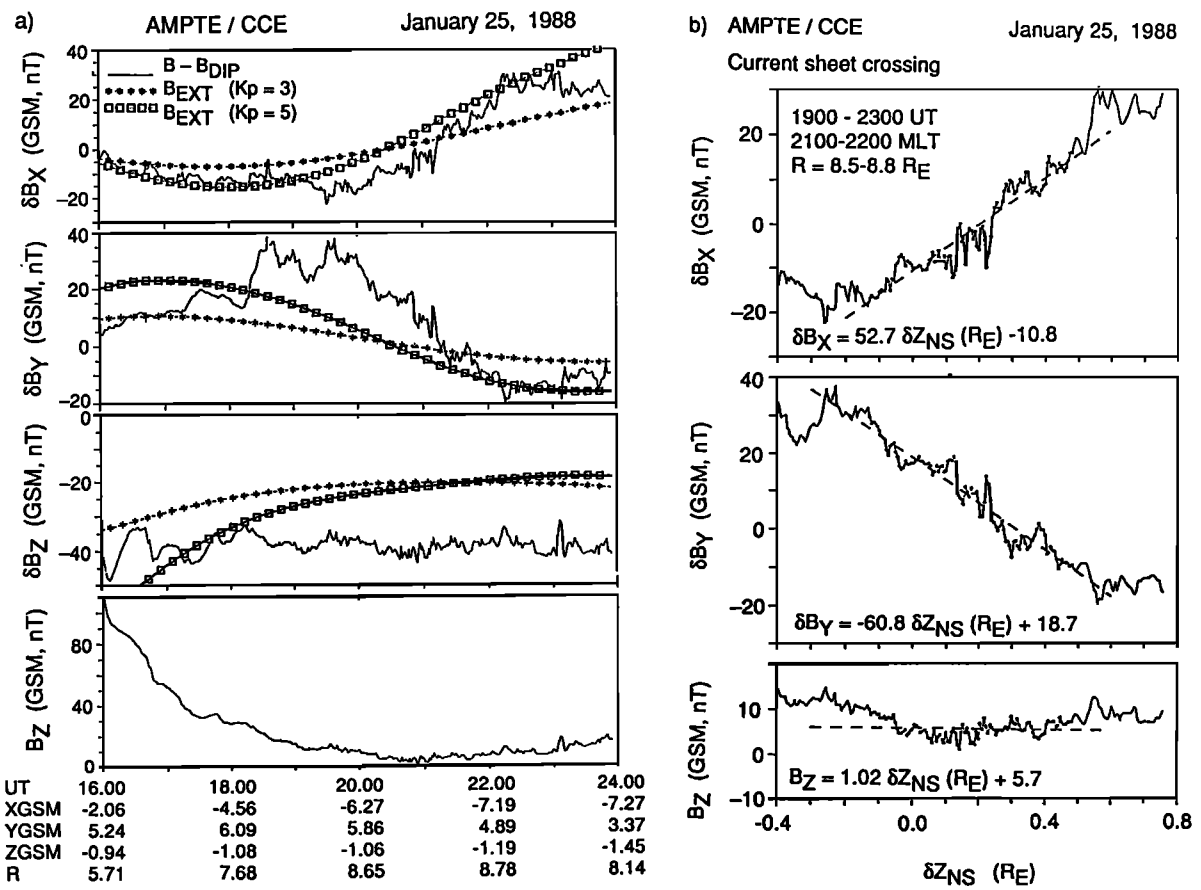

Figure 3. Magnetic field (in GSM coordinates) observed by AMPTE/CCE on 25 January, 1988. (a) Field values with the dipole field subtracted (δB_X, δB_Y, δB_Z), and the total B_Z are shown. For comparison, the first three panels show the T89 model field for $Kp = 3$ and $Kp = 5$ (stars and squares, respectively). (b) The observed magnetic variations as a function of the estimated distance from the center plane of the warped current sheet.

the 1930–2230 UT time interval the B_X and B_Y changes were much slower, showing that the current sheet was rather thin (the half-thickness was only about 0.4 R_E). The gradient of the tangential magnetic field component was very high, about 80 nT/R_E (about 53 nT/R_E and 61 nT/R_E for B_X and B_Y components, respectively). This is much larger than the value 40–50 nT/R_E found at 6.6 R_E during the substorm growth phase [*Fairfield and Zanetti*, 1989]. A linear regression fit (Figure 3b) to the average total B_Z gave only a 5.7 nT field in the center of the current sheet.

Thus, the very modest ground magnetic activity during this SMC event strongly contrasts the extraordinarily high magnetic field depression and current concentration in the near-Earth tail.

Modeling of the Magnetospheric Magnetic Configuration

In this section we describe the initial results of magnetic field modeling for the SMC-event on November 24, 1981. The primary goal of the modeling was to study the strongly stretched near-Earth magnetic field using the GOES 2 measurements. The global magnetic field configuration was modeled by modifying the *Tsyganenko* [1989a] field model. The current sheet thickness and the current intensity were varied to find the configuration that best reproduced the geostationary magnetic field measurements between 0000 UT and 1400 UT (for details of the model, see *Pulkkinen et al.* [1992]).

Because the SMC periods have particular characteristics also in the midtail region, we utilize information of the midtail magnetic field (at ~20 R_E) obtained during other SMC events studied by *Sergeev and Lennartsson* [1988]. They showed that the following characteristics are typical for midtail magnetic field during SMC periods: (1) The tail lobe magnetic field does not significantly deviate from its quiet-time value, and is described by T89 models with $Kp = 2$ or $Kp = 3$; (2) The current sheet half-thickness is about 4 R_E; and (3) B_Z in the plasma sheet center is 6–8 nT.

In the near tail, comparison of the magnetic field observations and the T89 model results shown in Figure 1 shows that the radial component was very large and the normal component was very depressed. These effects were modeled by a local thinning of the current sheet, and by an intensification of both the tail and ring current contributions in the T89 $Kp = 2$ model. Away from the midnight sector near the geosynchronous orbit the observed transition from the stretched taillike field to the quasi-dipolar field occurred much more rapidly than was predicted by the model. This discrepancy can be removed by adding a sufficiently strong azimuthal current to the model. We therefore introduced an additional current disc similar to the ring current in the T89 model [*see Pulkkinen et al.*, 1992].

Energetic particle data from low altitudes and the auroral images from the DE 1 spacecraft show that the oval was over 10° wide during this event [*Yahnin et al.*, 1994]. This suggests that a relatively large amount of magnetic flux crossed the the tail equatorial plane. This, in turn, suggests that the plasma sheet was expanded and that the normal component was relatively large in the midtail region. This conclusion is further supported by in situ magnetic field observations in the midtail during other SMC periods. The T89 field model predicts a very small magnetic field normal component in that region. In addition to the above modifications, we expanded the plasma sheet in the midtail region by a factor of 3. This produced a thicker current sheet and a somewhat larger normal component, about 5 nT at 15 to 20 R_E, which increased the amount of closed flux in the tail. With these features included, the model satisfied the midtail characteristics found by *Sergeev and Lennartson* [1988] listed above.

The parameters for the modified model were evaluated by a least squares fitting, using 3-min averages of the magnetic field measured by GOES 2 during 0000–1400 UT. The free parameters were the minimum current sheet thickness, the location and width of the thinned part of the current sheet, the net intensities of the tail and ring currents, and the intensity and characteristic radial variation of the additional current. The least squares error was minimized throughout this 7-dimensional space. The magnetic field configuration was assumed to remain static during the modeled period.

The best fit with the observed field was achieved when the current sheet was thinned to 20% of the T89 model value, the thinned region was centered at $X = -13$ R_E, and had a scale length of 12 R_E in the X direction (see

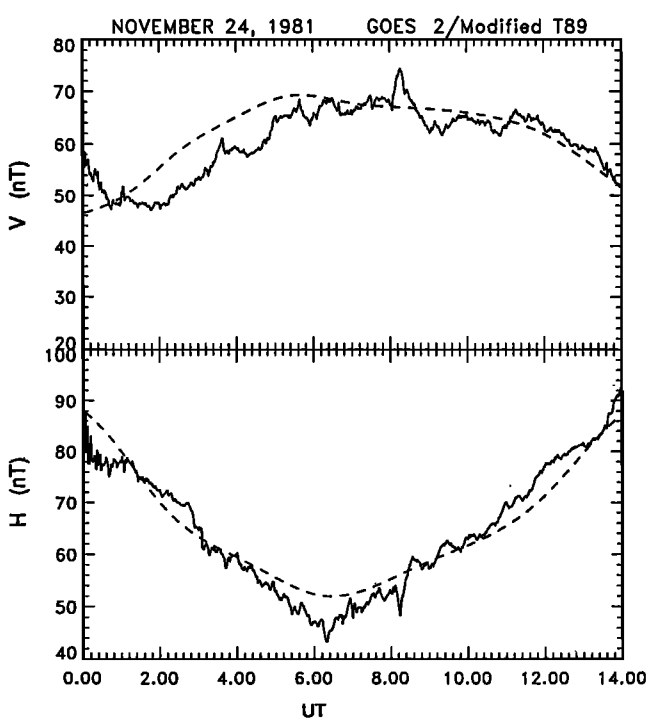

Figure 4a. Magnetic field measurements (H (vertical) and V (radial) components, geographic coordinates) from GOES 2 (solid lines) on November 24, 1981. The dashed lines show the field components computed using the modified T89 model described in the text.

Pulkkinen et al. [1992] for details of the model). The tail and ring currents were intensified by 10% and 20% from the corresponding T89 model values, respectively. The intensity of the additional current sheet was chosen 120% of that for the ring current in the T89 $Kp = 2$ model, and its radial scale size was $\sim 0.8\ R_E$ larger than the T89 model value. Figure 4a shows the radial (V) and normal (H) components of the observed magnetic field (solid line) and that in the modified model (dashed line). Note the much better agreement of the radial component in the modified model outside the midnight sector, as well as a very good fit of the normal component throughout all local times from 1700 MLT to 0700 MLT (compare with Figure 1, which shows the T89 model values).

The strong enhancement of the currents in the near-Earth region stretches the field lines tailward. The geodipole tilt angle was large during this event (about $-24°$), shifting the current sheet by $\sim 2\ R_E$ below the Sun-Earth line at $X = -6.6\ R_E$. Figure 4b shows the nightside magnetic field lines with ionospheric footpoints between 60° and 80° (corrected geomagnetic latitude, CGLat) at 2° intervals. For comparison, the original Tsyganenko model field lines are shown by the dotted lines.

The obtained model for the near-Earth magnetic field configuration much resembles that found during strong substorm growth phases. Earlier global modeling results [*Pulkkinen et al.*, 1992] have shown that during intervals with a moderate activity the growth-phase-associated currents flow mainly in the dawn-dusk direction and are located around $R \sim 10\ R_E$. However, during strong substorm growth phases, the currents may build up very close to the Earth (at geostationary distance and even closer), and in these cases the increased currents are nearly azimuthal [*Pulkkinen et al.*, 1991]. The current intensities obtained in the present case turned out to be close to those found during strong substorm growth phases. It thus seems that during periods of steady magnetospheric convection the near-Earth portion of the magnetotail remains stationary for many hours and its configuration is similar to that observed during the late substorm growth phase.

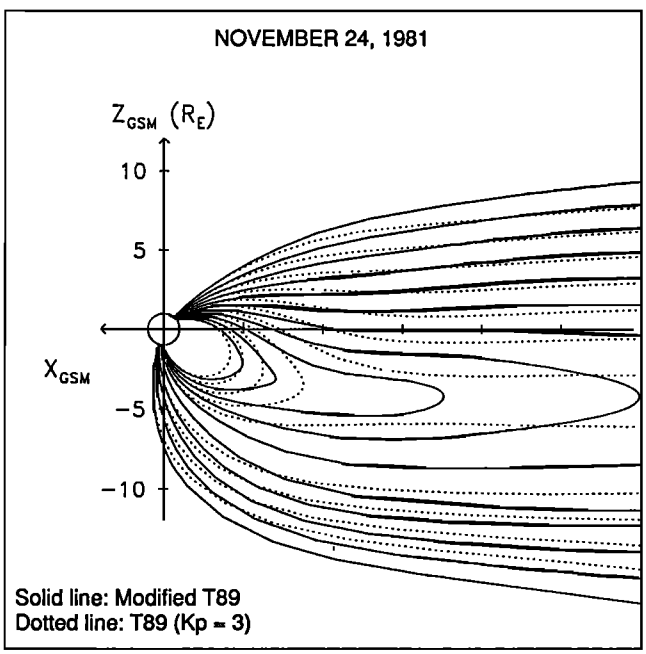

Figure 4b. Magnetic field line configuration according to the modified magnetospheric model (solid lines) and original T89 $Kp = 3$ model (dotted lines) for the November 24, 1981 event.

Table 1. Ionospheric Footpoints of Field Lines at the Midnight Meridian. Distances from the Earth are given in solar magnetospheric coordinates (GSM).

X_{GSM} R_E	Northern Hemisphere deg	Southern Hemisphere deg
6.6	63.0	-62.6
10	64.5	-64.1
20	66.2	-65.4
50	69.9	-69.2

To compare the tail model with the auroral observations, we mapped several field lines from the equatorial current sheet to the ionosphere. Table 1 shows the ionospheric footpoints of the midnight meridian field lines both for the northern and southern hemispheres. The differences between the two magnetic latitudes give a rough measure of the amount of the tilt-related asymmetry in the location of the conjugate points (in this event the tilt angle was $\Psi \approx -24°$).

Remote Sensing of the Equatorial Magnetic Field

The remote sensing technique is based on pitch-angle scattering of energetic particles bouncing between their mirror points at low altitudes. Particles are effectively scattered in the equatorial plane (and hence fill the loss cone) when

$$\frac{R_C}{\rho} = \frac{B_Z}{G}\frac{\delta B_X}{\delta Z} \leq 8 \qquad (1)$$

[*Sergeev and Tsyganenko*, 1982]. Here R_C and ρ are the radius of curvature of the magnetic field line and the particle gyroradius, respectively, and $G = mv/e$ is the particle rigidity. The boundary between the regions of adiabatic and nonadiabatic particle motion in the equatorial current sheet depends only on the equatorial magnetic field and the particle rigidity. At low altitude, this boundary corresponds to the boundary between the regions of empty and filled loss cone pitch-angle distributions (isotropic boundary, or IB). Therefore, detection of the isotropic boundary at low altitudes for particles of given rigidity implies that equation (1) (with the equality sign) is satisfied in the equatorial cross section of the corresponding magnetic flux tube. Thus, this method can be used for predicting the high-altitude equatorial magnetic field when the low-altitude precipi-

tation patterns for different energies as a function of latitude are known. Alternatively, a model magnetic field can be used to calculate the predicted lowest latitude where isotropic particle distributions for given energies are expected to be found.

This pitch-angle scattering mechanism has been discussed and tested in several papers. *West et al.* [1978] used Ogo 5 energetic particle and magnetic field data during several quiet-time inbound passes in the equatorial regions of the tail. They found good agreement between the isotropic boundary positions observed in the energetic particle data and the boundaries predicted by using a magnetic field model based on the in situ magnetic field observations. The consistency of the energetic particle morphology at low altitudes with the mechanism of the particle scattering in the tail current sheet has also been also confirmed (cf. discussion and references in *Imhof* [1988] and in *Sergeev et al.* [1993]). Finally, the isotropic boundary algorithm (IBA) for remote sensing of the equatorial magnetic field was suggested and successfully tested [*Sergeev et al.*, 1993] by using simultaneous observations of the isotropic boundary positions determined using particle data from low-altitude NOAA-type spacecraft and magnetic field measurements onboard geostationary spacecraft GOES 2.

The NOAA 6 and NOAA 7 spacecraft were in orbit during the SMC event on November 24, 1981, introduced earlier in Figures 1 and 4. Both satellites carried similar instruments for measuring fluxes of trapped and precipitating energetic particles in several energy bands. (Proton channels for energies $\geq$30, $\geq$80, and $\geq$250 keV are denoted as P1, P2, P3, and the electron channels for energies $\geq$30, $\geq$100, and $\geq$300 keV are denoted as E1, E2, E3, respectively.) In addition, the total precipitated energy flux of ions and electrons at auroral energies (0.3–20 keV) was measured. Details of the global particle morphology and the boundaries for this SMC event have been discussed earlier by *Yahnin et al.* [1994]. Here we concentrate only on the passes that occurred close to magnetic midnight (2200–0200 MLT) between 0400 and 1000 UT, when GOES 2 was near magnetic midnight in the near-Earth tail.

Figure 5a shows low-altitude particle observations on November 24, 1981, 0817–0822 UT. The auroral oval was very wide, extending from 61° to 70° (CGLat). The transition from the empty loss cone (low ratio of precipitating to trapped particle fluxes) to isotropic precipitation is well defined for all energy channels except for E1, and all transitions occurred in the equatorward part of the oval (between 61° and 64°). In the E1 channel (electrons with $E \geq 30$ keV) the particle distributions isotropized also in this low-latitude region. However, poleward of that, the precipitating fluxes at higher latitudes fell below the level of the trapped fluxes and then returned back several times. In this case, the lowest latitude occurrence of the isotropic fluxes was assumed to indicate the isotropic boundary position.

The plots of the observed isotropic boundary latitudes as a function of particle rigidity for all orbits that passed close to midnight between 0400 and 1100 UT are shown in Figure 5b. The surprising similarity of the profiles is clear evidence of a very stable magnetospheric configuration [see also *Yahnin et al.*, 1994]. Comparison with the isotropic boundary profiles computed using $Kp = 4$ and $Kp = 5$ T89 models and equation (1) shows that only the highly disturbed field model can predict the observed low latitudes of isotropic precipitation. Furthermore, the experimental profiles are much steeper than the ones obtained from the model. This disagreement is typical; very steep observational profiles are quite common [cf. *Imhof*, 1988]. Qualitatively, this means that the amount of magnetic flux between the isotropic boundary L shells, for any two rigidities satisfying equation (1), is much less than that predicted by the model. In other words, the profiles suggest a very depressed equatorial magnetic field and/or a much larger vertical magnetic field gradient. Both conclusions are in qualitative agreement with the magnetic field observations in the previous section.

The isotropic boundary profile of the energetic particles provides an independent test for the global magnetic field model developed in the previous section. Figure 5c shows the profile obtained by averaging all the near-midnight profiles given in Figure 5b. Similar to Figure 5b, the two dashed lines show the profiles derived from the T89 model for two different Kp values. The line with circle symbols shows the modified T89 model result. Both the location and shape of the isotropic boundary are well predicted by the modified model. Note that even though the currents were strongly enhanced in the near-Earth region, the observed profile is still steeper than that predicted by the model, implying that even stronger magnetic field gradients could be present near the midnight sector of the tail. Comparison of this global model with the AMPTE/CCE observations on January 25, 1988 (Figure 3), shows that at $X \sim 8.8\ R_E$ the model B_Z is $\sim$ 13 nT at the current sheet center, whereas the CCE results showed that the field was as small as 5 nT. This further emphasizes the strong gradients in B_Z that may develop along the tail axis during SMC events.

Discussion

Low AE and Kp Values During the SMC Events

At first sight, it seems paradoxical that even if the tail magnetic field is very disturbed, the widely used activity indices Kp and AE are low and unable to properly respond to the disturbances observed in the tail field during the SMC events. However, detailed analysis of the indices shows that during these untypical conditions such behavior is to be expected.

Kp represents a measure of the variation amplitude of the geomagnetic field at midlatitudes. During SMC events the solar wind flow is steady (i.e., produces no sudden impulselike variations at midlatitudes) and there are no strong variations of field-aligned currents that would give rise to magnetic bays typically observed during substorms. Thus the midlatitude magnetic field

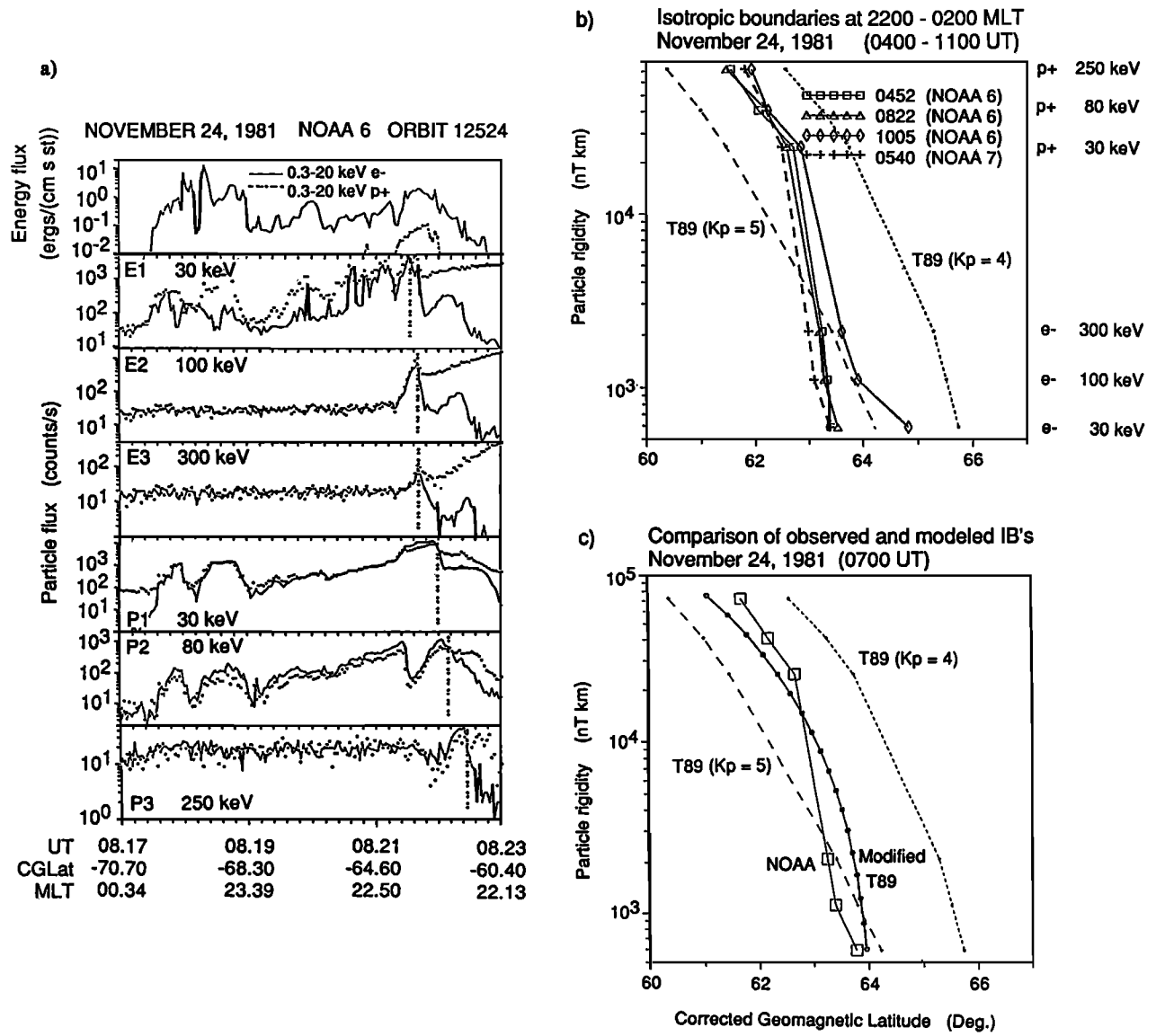

Figure 5. (a) Particle observations from NOAA 6 and NOAA 7 low-altitude spacecraft on November 24, 1981. Top panel: The latitudinal profile of the total particle flux near magnetic midnight. The electron and proton fluxes are shown separately (solid and dashed lines, respectively). The following six panels show the corresponding fluxes for the different energy channels (three electron channels for energies $\geq$30, $\geq$100, and $\geq$300 keV (E1, E2, E3), and three proton channels for energies $\geq$30, $\geq$80 and $\geq$250 keV (P1, P2, P3)). The precipitated particle fluxes are shown by the solid lines, and the trapped particle fluxes by the dotted lines. (b) Latitudinal profiles of the isotropic boundaries for different rigidities observed during several near-midnight passes of NOAA spacecraft on November 24, 1981. The model profiles obtained by using equation (1) and the T89 magnetic field models for $Kp = 4$ and $Kp = 5$ are also shown. c) Average latitudinal profile of the isotropic boundaries at different rigidities on November 24, 1981. This profile was obtained by averaging over the four individual profiles shown in Figure 5b. The solid line with small circles shows the modified T89 model; the dashed lines show the T89 models for $Kp = 4$ and $Kp = 5$.

shows only a smooth daily variation, naturally resulting in low Kp values. On the other hand, the AU/AL indices are proportional to the linear current density of the eastward/westward auroral electrojets. However, the total electrojet current depends on the latitudinal width of the electrojets. Because the typical latitudinal width of the nightside oval during SMC events is ~10° (see *Yahnin et al.* [1994] and Figure 5a), the total electrojet current may be 2–3 times higher than during non-SMC periods for the same AE value.

The discrepancy between the low ionospheric activity level (as measured by Kp and AE) and the disturbed tail field has been earlier reported by *West et al.* [1978], who demonstrated cases of a surprisingly taillike magnetic field at 8–15 R_E during very quiet ionospheric conditions. This together with the SMC event obser-

vations leads to an important practical conclusion: the ground activity indices do not always give a good measure of the magnetospheric activity.

No such problems are expected for the *Dst* index. Its relatively disturbed values (about −60 and −80 nT for the events in Figures 1 and 2, respectively) reflect the very intense current in the near-Earth tail found in the spacecraft observations and in our modeling study. However, according to our experience, a disturbed value of *Dst* is neither a sufficient nor necessary condition for an SMC event.

Two Different Regions in the Plasma Sheet

Figure 6a displays the radial dependence of the total model magnetic field in the central plane of the current sheet along the midnight meridian (denoted as B_N, because the current sheet is very warped and the corresponding field component is thus directed along the local normal to the current sheet surface). Unlike the monotonous B_N profile in the T89 model, our modeling gave a nonmonotonous profile, which helps to identify two different plasma sheet regions in the tail. The depth

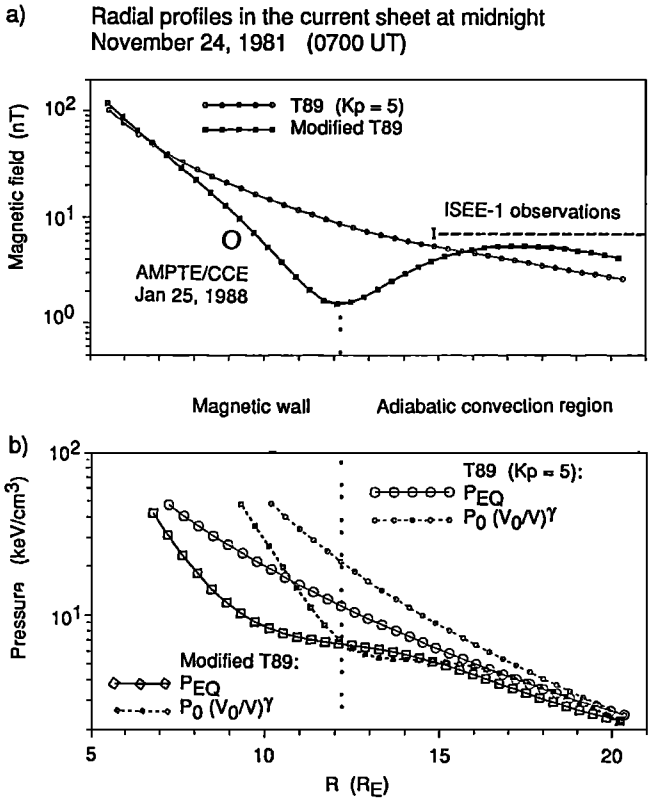

Figure 6. (Top) Total magnetic field in the central surface of the current sheet at midnight as a function of radial distance from the modified model developed in text (thick line with squares) and from the T89 model for $Kp = 5$ (thin line, open circles). The observations by AMPTE/CCE (from Figure 3, large open circle) and by ISEE 1 (from *Sergeev and Lennartsson* [1988], long dashed line) are shown for reference. (Bottom) The radial profiles of the equilibrium and adiabatic pressures (see text) computed using the modified T89 model (thick lines, squares) and using the T89 model for $Kp = 5$ (thin lines, circles).

of the minimum (and to some extent its location) are dependent on the expansion of the model midtail current sheet, which was done based on previous observations rather than in situ measurements in this particular event. However, even a model without the midtail current sheet expansion produces a (smaller) minimum in B_N due to the strong enhancment of the currents and thinning of the near-Earth current sheet.

The region Earthward of the B_N minimum is characterized by the large radial gradient in the magnetic field, and we thus call it the "magnetic wall." Strong currents flow in this region, and large current densities, large magnetic gradient drift velocities, and large pressure gradients are expected to exist. Outside the weak-field region near the magnetic field minimum, particle motion is expected to be nearly adiabatic. This may allow the formation of a significant pressure anisotropy, which could sustain the very thin current sheet. The anisotropy may develop due to several mechanisms, e.g., those resulting from drift shell splitting and particle losses at the dayside magnetopause [*Tsyganenko*, 1989b].

This near-Earth region was the main object of our global magnetic field modeling, as it was covered by in situ spacecraft measurements. The existence of the steep gradient was quantitatively confirmed by using the isotropic boundary profiles obtained from the low-altitude spacecraft data (see Figure 5c). Actually, the B_N profile may have been even steeper at $R \sim 7$–9 R_E than was predicted by the model. This is suggested by the steeper experimental isotropic boundary profile at 63°–64° in Figure 5c. The low B_N values measured by AMPTE/CCE at 8.8 R_E in another SMC event on January 25, 1988, (shown by the circle in Figure 6a) give further support for the conclusion.

Tailward of the B_N minimum the field is characterized by a flat B_N profile (weak gradient) or even by increasing B_N as the radial distance increases (as demonstrated in our model). The latter feature is associated with a local minimum of B_N (at ~12 R_E in our model). We refer to this region tailward of the field minimum as the "adiabatic convection region." This region was not covered by in situ observations in the event we modeled, and thus our model results cannot be considered definitive. However, there is both direct and indirect evidence that support the existence of this region of adiabatic convection. Note that although the convection flow is adiabatic, the individual ion trajectories show nonadiabatic characteristics.

The magnetic field measurements during the SMC events support both the deep minimum in the near-Earth field and the relatively large value in the midtail. Earthward of the adiabatic convection region, we in one event directly measured $B_N \sim 5$ nT at 8.8 R_E (Figure 3). The continuing steep decrease of B_N makes it quite believable that B_N was even smaller somewhat tailward of the AMPTE/CCE apogee. Within the region of adiabatic convection in the plasma sheet (~20 R_E near midnight), the average B_N value can be as high as 6–8 nT. This result was earlier reported by *Sergeev and*

Lennartsson [1988], based on ISEE 1 data during several SMC events; they also emphasized that there was no obvious radial gradient of B_N between 15 and 20 R_E. Their experimental B_N value is also shown in Figure 6a.

The large latitudinal width of the nightside auroral oval (~10° wide, poleward boundary at ~70°–72° CGLat) implies that a large amount of magnetic flux crosses the plasma sheet, which further supports the observed large plasma sheet field values in the event we have modeled. Magnetic mapping of the oval boundaries gives an estimate of the length of the tail during SMC periods. In our model, B_N was ~5 nT at $R \sim 15 - 20$ R_E, which resulted in mapping of the suggested location of the last closed field line (100 R_E [*Slavin et al.*, 1985]) to about 72° CGLat. This approximately fits the observed position of the poleward boundary of the auroral oval, although caution is necessary when applying the model at such large distances. In general, B_N must be relatively large ($\geq$5 nT) at least from 15 to 25 R_E, in order to have the field line from 100 R_E to reach the Earth at $\geq$70° CGLat. Thus, $B_N \sim 6-8$ nT given by *Sergeev and Lennartsson* [1988] should be a well representative field value at distances of 15–20 R_E.

The behavior of energetic particle fluxes shown in Figure 5a shows several interesting features. We already noted that unlike in the other channels, the 30-keV electrons displayed a variable pattern with precipitated fluxes sometimes below and at other times at the level of trapped fluxes poleward of the isotropic boundary. In terms of the current sheet scattering mechanism, such a pattern suggests that for most of the magnetic flux tubes tailward/poleward of the isotropic boundary the current sheet field B_N is close to and fluctuates around its threshold level. For the 30-keV electrons the threshold is about 5 nT [cf. *Sergeev et al.*, 1993]. Similarly, the steadily isotropic fluxes of higher-rigidity (higher-energy) particles in the poleward half of the oval (having higher threshold B_N values, in excess of 10 nT) imply that B_N is $\leq$ 10 nT tailward of 10 R_E distance. Thus the energetic particle pattern confirms the deep local minimum of B_N at the interface between the two regions and is compatible with the observed and modeled values of $B_N \sim$ 6–8 nT at 15–20 R_E. (Precipitation caused by particle scattering by plasma instabilities cannot, of course, be either excluded or checked in our case. Here we discuss these observations only in terms of the chaotic scattering in the current sheet.)

The plasma sheet region characterized by adiabatic convection has very different physical properties than the magnetic wall region with steep radial magnetic field gradients. In the adiabatic convection region a large portion of the thermal protons are in chaotic orbits, and the plasma pressure is thus nearly isotropic. This, in turn, is consistent with the thick current sheet (half-thickness about 4 R_E) found at 15–20 R_E [*Sergeev and Lennartsson*, 1988]. Due to the weak magnetic field gradient, magnetic drifts are relatively weak and plasma sheet current densities are rather small. The weak (or even reversed) $\partial B_N/\partial R$ implies only a small change in the volume of the convecting magnetic flux tubes, which results in little or no compression and heating of the plasma.

Pressure Balance Problem During the Steady Convection

We can estimate the equilibrium plasma pressure in the current sheet from the quantitative field model for the steady convection event developed above. Because the isotropic pressure approximation is reasonably accurate for the region of adiabatic convection, the force balance condition

$$\nabla P = \mathbf{j} \times \mathbf{B} \tag{2}$$

may be integrated to give

$$P_{EQ}(R) = P_0 + \int_{R_0}^{R} j_Y \; B_N \; dR, \tag{3}$$

where the integration is done along the intersection line between the central surface of the current sheet and the midnight meridian. By choosing the initial point in the current sheet center at $R_0 = 20.5$ R_E and taking the initial pressure value P_0 to be in balance with the lobe magnetic pressure ($P_0 = {B_{TOT}}^2/2\mu_0$, where B_{TOT} was evaluated from the model at $X = -20$ R_E and $Z = 8$ R_E), we may compute B_N and j_Y ($\mu_0 \mathbf{j} = \nabla \times \mathbf{B}$) from the model and, finally, integrate equation (3) to obtain P_{EQ}. This simple procedure has been previously used by several authors to estimate the equilibrium pressure profile [*Kan et al.*, 1992; *Sergeev* 1990]. Starting from $R = R_0$ we also computed the volume (V) of the unit magnetic flux tube and the plasma sheet pressure expected from the adiabatic plasma compression from $P_{AD} = P_0(V_0/V)^\gamma$ with $\gamma = 5/3$. Note that the adiabatic compression approximation is not valid in the magnetic wall region [see *Erickson*, 1992], which limits the following comparison between P_{AD} and P_{EQ} to the adiabatic convection region.

The results from our model computations are given in Figure 6b. Starting from $R_0 = 20.5$ R_E (where $P_{AD} = P_{EQ} = P_0$ by definition) and using the original T89 model we obtain a pressure unbalance at the inner boundary of the adiabatic convection region ($X = 12$ R_E), $P_{AD}/P_{EQ} \sim 2$ (small and large circles in Figure 6b). When the computation was done using the field model developed for the SMC event, there is no unbalance between P_{AD} and P_{EQ} within the adiabatic convection region. Thus there is no notable pressure balance inconsistency during the steady convection period. This is due to the very peculiar but stable magnetic configuration proposed to exist during the SMC events.

This type of field configuration for steady adiabatic convection has been earlier theoretically predicted by several authors [*Hau et al.*, 1989; *Hau*, 1991; *Erickson*, 1992]. For example, Hau et al. found several equilibrium solutions, where the magnetic field minimum was at about 12 R_E and the depth of the minimum was

about 20% of the maximum field in the midtail current sheet. These numbers are very close to what we found in our analysis. The basic difference in our model and the Hau et al. equilibria is that in our model the minimum is more localized in radial distance: In the Hau et al. model there is a negative magnetic field gradient over about 15 R_E, whereas in our model the negative field gradient is localized between 12 and 17 R_E.

Conclusions

1. We demonstrated, using various observations and magnetic field modeling, that during long active periods between substorms (the SMC events) the magnetic configuration in the near-Earth tail is very stressed, while the midtail plasma sheet is thick and has a large normal magnetic field component. In spite of the very moderate level of ground magnetic activity displayed by AE and Kp, the magnetic field is very taillike in the near-tail region: thin stable current sheet of less than 1 R_E scale thickness is sustained. The magnetic field in the current sheet center is very depressed and may be as small as ~5 nT even inside 10 R_E. This results in very large magnetic field gradients at radial distances 5–10 R_E, which may effectively contribute to the escape of particles due to their fast azimuthal drift and/or chaotic acceleration from the Earthward moving flux tube.

2. We found strong evidence for the approximately equal magnetic field values in the current sheet at 8–9 R_E and in the midtail at 15–20 R_E (as reported by *Sergeev and Lennartsson* [1988]) and an indication of a local minimum in the radial B_N profile at about 12 R_E. The resulting magnetic configuration appears to be very close to that required to maintain steady state convection in the plasma sheet [*Hau*, 1991; *Erickson*, 1992]. The excess pressure increase that would occur during flux tube convection from $R = 20$ R_E to $R = 12$ R_E in a monotonically decreasing magnetic field profile (and thus give rise to the pressure imbalance) seems to be basically removed due to the peculiar magnetic configuration. This result supports the good predictive capability of the MHD approach and supports the pressure balance inconsistency model for the substorm growth phase.

3. Our results raise, however, a new problem: how can such a stressed configuration with such a thin and intense current sheet in the near-Earth tail (resembling the substorm growth phase) remain stable during many hours? More extensive studies are required to shed light on the current sheet stabilization and the mechanisms which trigger the current disruption and lead to the substorm expansion.

Acknowledgments. Particle data from NOAA spacecraft and magnetic data of GOES 2 spacecraft used in this study were obtained through WDC-A for STP in Boulder. The data from AMPTE/CCE were obtained through NSSDC for Rockets and Satellites, at NASA/GSFC. We thank Dr. M. Sugiura and Dr. T. Kamei from WDC-C2 in Kyoto for providing the *Dst* index data. We also thank Dr. T. Bösinger for his help in providing us with the NOAA spacecraft data. This work is a continuation of the joint Russian-Finnish project which was supported by the former Soviet-Finnish working group on geophysics. V.A.S. thanks the Academy of Finland for financial support. N.A.T. acknowledges the National Research Council Award granted for holding a Research Associateship at NASA/GSFC.

The Editor thanks Gary M. Erickson and another referee for their assistance in evaluating this paper.

References

Ashour-Abdalla, M., L. M. Zelenyi, and J.-M. Bosqued, The formation of the wall region: Consequences in the near-Earth magnetotail, *Geophys. Res. Lett., 19*, 1739, 1992.

Erickson, G. M., A quasi-static magnetospheric convection model in two dimensions. *J. Geophys. Res., 97*, 6505, 1992.

Erickson, G. M., and R. A. Wolf, Is steady convection possible in the Earth's magnetotail? *Geophys. Res. Lett., 7*, 897, 1980.

Fairfield, D. H., and L. J. Zanetti, Three-point magnetic field observations of substorms in the inner magnetotail, *J. Geophys. Res., 94*, 3565, 1989.

Hau, L. N., Effects of steady state adiabatic convection on the configuration of the near-Earths plasma sheet, 2, *J. Geophys. Res., 96*, 5591, 1991.

Hau, L. N., R. A. Wolf, G.-H. Voigt, and C. C. Wu, Steady-state magnetic field configurations for the Earth's magnetotail, *J. Geophys. Res., 94*, 1303, 1989.

Imhof, W. L., Fine resolution measurements of the L-dependent energy threshold for isotropy at the trapping boundary, *J. Geophys. Res., 93*, 9743, 1988.

Kan, J. R., W. Sun, and W. Baumjohann, A hybrid equation of state for the quasi-static central plasma sheet, *Geophys. Res. Lett., 19*, 421, 1992.

Lui, A. T. Y., R. E. Lopez, B. J. Anderson, K. Takahashi, L. J. Zanetti, R. W. McEntire, T. A. Potemra, D. M. Klumpar, E. M. Greene, and R. Strangeway, Current disruptions in the near-Earth neutral sheet region, *J. Geophys. Res., 97*, 1461, 1992.

Pontius, D. H., and R. A. Wolf, Transient flux tubes in the terrestrial magnetosphere, *Geophys. Res. Lett., 17*, 49, 1990.

Pulkkinen, T. I., D. N. Baker, D. H. Fairfield, R. J. Pellinen, J. S. Murphree, R. D. Elphinstone, R. L. McPherron, J. F. Fennell, R. E. Lopez, and T. Nagai, Modeling the growth phase of a substorm using the Tsyganenko model and multispacecraft observations: CDAW-9, *Geophys. Res. Lett., 18*, 1963, 1991.

Pulkkinen, T. I., D. N. Baker, R. J. Pellinen, J. Büchner, H. E. J. Koskinen, R. E. Lopez, R. L. Dyson, and L. A. Frank, Particle scattering and current sheet stability in the geomagnetic tail during the substorm growth phase, *J. Geophys. Res., 97*, 19283, 1992.

Sergeev, V. A., Problems in simulation of convection in the plasma sheet (in Russian), in *Magnetospheric Researches, vol 17*, edited by V. S. Semenov, p.3, National Geophysical Committee, 1990.

Sergeev, V. A., and W. Lennartsson, Plasma sheet at $X \sim -20$ R_E during steady magnetospheric convection, *Planet. Space Sci., 36*, 353, 1988.

Sergeev, V. A., W. Lennartsson, R. Pellinen and M. Vallinkoski, Average patterns of precipitation and plasma flow in the plasma sheet flux tubes during steady magnetospheric convection, *Planet. Space Sci., 38*, 355, 1990.

Sergeev, V. A., and N. A. Tsyganenko, Energetic particle losses and trapping boundaries as deduced from calculations with a realistic magnetic field model, *Planet. Space Sci., 30*, 999, 1982.

Sergeev, V. A., M. Malkov, and K. Mursula, Testing the isotropic boundary algorithm method to evaluate the magnetic field configuration in the tail, *J. Geophys. Res., 98*, 7609, 1993.

Slavin, J. A., E. J. Smith, D. G. Sibeck, D. N. Baker, R. D. Zwickl, and S.-I. Akasofu, An ISEE 3 study of average and substorm conditions in the distant magnetotail, *J. Geophys. Res., 90*, 10,875, 1985.

Spence, H. E., and M. G. Kivelson, The variation of the plasma sheet polytropic index along the midnight meridian in a finite width magnetotail, *Geophys.Res. Lett., 17*, 591, 1990.

Tsyganenko, N. A., On the convective mechanism for formation of the plasma sheet in the magnetospheric tail, *Planet. Space Sci., 30*, 1007, 1982.

Tsyganenko, N. A., Magnetospheric magnetic field model with a warped tail current sheet, *Planet. Space Sci., 37*, 5, 1989a.

Tsyganenko, N. A., On the re-distribution of the magnetic field and plasma in the near nightside magnetosphere during a substorm growth phase, *Planet. Space Sci, 37*, 183, 1989b.

West, H. I., Jr., R. M. Buch, and M. G. Kivelson, On the configuration of the magnetotail near midnight during quiet and weakly disturbed periods: State of the magnetosphere, *J. Geophys. Res., 83*, 3805, 1978.

Yahnin, A. G, et al., Features of steady magnetospheric convection. *J. Geophys. Res., 99*, 4039, 1994.

R. J. Pellinen and T. I. Pulkkinen, Finnish Meteorological Institute, P.O.Box 503, SF-00101 Helsinki, Finland. (e-mail: risto.pellinen@fmi.fi, tuija.pulkkinen@fmi.fi)

V. A. Sergeev, Institute of Physics, University of St. Petersburg, 198904 St. Petersburg, Russia. (e-mail: sergeev@solar.phys.lgu.spb.su)

N. A. Tsyganenko, NASA/GSFC, Code 695, Greenbelt, MD 20771. (e-mail: lepvax::ys2nt)

(Received June 30, 1993; revised August 23, 1993; accepted July 28, 1994.)